JOURNAL OF CATALYSIS 103, 302–310 (1987)

The Oxidative Conversion of Methane to Higher Hydrocarbons

JOHN A. SOFRANKO,[1] JOHN J. LEONARD, AND C. ANDREW JONES

ARCO Chemical Company, A Division of Atlantic Richfield Company, 3801 West Chester Pike, Newtown Square, Pennsylvania 19073

Received April 8, 1986; revised August 18, 1986

Many transition metal oxides have been evaluated as oxidative coupling catalysts for converting methane to C_2 and higher hydrocarbons. Reactions were done in a cyclic redox mode in which oxidized catalyst was reacted with methane in the absence of oxygen to form coupling products and reduced catalyst which was reoxidized with air in a separate step. Manganese, indium, germanium, antimony, tin, bismuth, and lead oxides were found to be effective coupling catalysts, giving 10 to 50% selectivity to higher hydrocarbons. Silica is a superior support compared to alumina. Mechanistic studies with manganese oxide on silica indicate that the initial coupling product is ethane which is formed via dimerization of a CH_3 radical-like species. The ethane is oxidatively dehydrogenated to ethylene which may react with CH_3 to give propylene. The major path for combustion involves sequential oxidation of products. © 1987 Academic Press, Inc.

INTRODUCTION

The conversion of natural gas to an easily transportable liquid fuel, particularly in remote areas of the world, is becoming an important challenge. This has, of course, been an active technical area for at least 50 years. Early commercial attempts (*1*) concentrated on direct thermal conversion. Respectable liquid yields were obtained but thermal routes were very inefficient due to the endothermicity of the process. With the advent of catalytic steam reforming in the 1930s, the conversion of synthesis gas via Fischer–Tropsch catalysis became the most practical method of gas conversion. The oil embargoes of the early 1970s sparked renewed interest in synthesis gas chemistry.

Two major limitations of Fischer–Tropsch chemistry still exist. Steam reforming of methane is an energy- and capital-intensive process. In addition, long-term synthesis catalyst performance avoiding the Schulz–Flory product distribution has not been demonstrated. The most promising method to avoid the Schulz–Flory limitations is via methanol conversion over shape selective zeolites. However, steam reforming and methanol synthesis are still required. An important chemical challenge is to convert natural gas, principally methane, to liquid fuels in a simple, energy-efficient reaction scheme. The goal of this work is the direct one-step conversion of methane to higher molecular weight hydrocarbons over metal oxide redox agents.

Direct conversion of methane to higher hydrocarbons plus hydrogen, Eq. (1), has severe thermodynamic limitations below

$$nCH_4 \rightarrow C_nH_{4n-2y} + yH_2 \qquad (1)$$

1500°K. At temperatures above 1500°K and at short contact times, high selectivities to acetylene are achievable as shown by the work of Happel and Kramer (*2*). In an oxidative system, Eq. (2), where water rather than hydrogen is coproduced,

$$nCH_4 + y/2O_2 \rightarrow C_nH_{4n-2y} + yH_2O \qquad (2)$$

there are no thermodynamic constraints. This was clearly realized by workers at Exxon (*3*) and Union Carbide (*4*).

The Exxon work claims a multimetal ox-

---

[1] To whom correspondence and reprint requests should be addressed.

0021-9517/87 $3.00

ide catalyst system containing a noble metal. The Union Carbide work describes a broad screening program involving single metal oxides. In many of the Union Carbide experiments, the reactor walls contributed to methane conversion. Both of these studies employed a cyclic or redox approach to methane oxidation. The catalyst lattice oxygen was the source of oxidizing equivalents for methane, Eq. (3), converting methane to higher hydrocarbons plus water:

$$n\mathrm{CH}_4 + \mathrm{MO}_{z+y} \rightarrow \mathrm{C}_n\mathrm{H}_{4n-2y} + y\mathrm{H}_2\mathrm{O} + \mathrm{MO}_z. \quad (3)$$

The reduced redox agent was then regenerated with air or an oxygen-containing gas in the absence of methane. Prior to publication of the Union Carbide work, a targeted redox screening program had been initiated using a functional approach to identify metal oxide candidates (5). This paper reports the results of this screening program. Higher yields of ethylene, ethane, and higher hydrocarbons than previously reported are observed, primarily due to a unique metal oxide–support interaction. Products as heavy as toluene are observed. Detailed characterization of the manganese redox catalyst system and preliminary mechanistic work are presented.

EXPERIMENTAL

Catalyst preparation. The catalysts for the screening study were all prepared on high purity silica, Houdry HSC 534, that has an initial surface area of 250–275 m^2/g. The catalysts were prepared by incipient wetness impregnation with aqueous solutions of the metal acetates or nitrates. They were impregnated to give nominally 5 wt% metal loadings. These were calcined in air at 800°C for 16 hr.

Reactor apparatus. The catalysts, 10 ml of 14- to 30-mesh pellets, were charged to 14-mm-i.d. quartz tubes. It should be noted that stainless-steel (310 or 316) is not sufficiently inert under these reaction conditions. The reactor tubes were electrically heated to reaction temperatures under a flow of air. In a typical redox sequence the air was purged from the reactor with nitrogen before the methane sequence began. Methane conversion runs were typically of 2 to 30 min in length. During this time instantaneous, or on-line, samples were taken. The total cumulative effluent was also collected in a gas bag. The end of the methane run was followed by a nitrogen purge. The redox agent was then reoxidized with air at reaction temperature. This also served to burn off carbonaceous material. The regeneration gases were also collected in a gas bag so that a coke yield could be calculated.

GC methods. The product effluents were analyzed for carbon monoxide, carbon dioxide, hydrogen, and methane on a TCD-GC. The column used for this one-injection analysis was a composite molecular sieve/Porapak CTR column from Alltech Associates, Inc., Deerfield, Illinois. The hydrocarbon products up to and including toluene were analyzed on a Porapak Super-Q column in an FID-GC. The carbon oxides formed upon regeneration were included in the total product yields that were summed to give the methane conversion. Results are reported on a carbon mole percentage basis. It should be noted that yield is defined as conversion times selectivity. The literature in this area contains many examples of the erroneous and misleading use of the term yield to mean selectivity.

RESULTS AND DISCUSSION

Screening Program

A metal oxide reagent may provide a kinetic pathway for thermodynamically possible reactions by oxidation of methane to higher hydrocarbons and water. While it may be desirable to develop a continuous process without the need for catalyst regeneration, this can only be done by including oxygen in the feed to constantly replenish the lattice oxygen. A number of studies with different metal oxides report the formation of methanol, formaldehyde, carbon

TABLE 1

Oxides Screened[a]

Oxide	Function[b]
Cr_2O_3	A, B, C, D
Mn_2O_3/Mn_3O_4	B, C, D
Bi_2O_3	A, B, C
Tl_2O_3	A, B, C
In_2O_3	A, B, C
PbO_2/PbO	A, B, C
PdO	A, B, C
Sb_2O_3	A, B, C
GeO_2	A, B, C
MoO_3	A, B, C
PtO	B, C, D
WO_3	B, C, D
U_3O_8	A, B
V_2O_5	A, B
CuO	B, C
SeO_2	B
TeO_2	B

[a] At 860 methane GHSV over 5 wt% metal on SiO_2 at 200–800°C.
[b] See text.

monoxide, and carbon dioxide from methane–oxygen feeds (*6*), but higher hydrocarbons either are not formed or are converted much faster than methane. More recently, work by Hinsen and Baerns (*7*), Ito *et al.* (*8*), and Otsuka *et al.* (*9*) does show the catalytic conversion of methane to higher hydrocarbons and carbon oxides.

To avoid overoxidation of products by gas phase oxygen, the source of oxidation activity must be lattice oxygen of the metal oxide. This scheme would consist of methane reaction followed by air regeneration of the catalyst.

The desired methane conversion catalyst must be multifunctional. First, it must activate methane. Second, it must allow coupling of transient, active hydrocarbon fragments. Third, it must be regenerable. Based on these considerations, it seemed that the desired metal oxide should be capable of one or more of the following four functions:

A. Oxidative dehydrogenation of paraffins to olefins or aromatics with concomitant formation of water (not hydrogen) in the absence of molecular oxygen. The oxide must be reoxidizable with air.

B. Oxygen atom transfer to hydrocarbons to give useful oxidized hydrocarbon products in the absence of molecular oxygen. The oxide must be reoxidizable with air.

C. Oxidative coupling of hydrocarbons with concomitant formation of water in the absence of molecular oxygen. Air regeneration is possible. Examples include conversion of toluene to stilbene and propylene to hexadiene or benzene.

D. Activation of methane as evidenced by hydrogen–deuterium exchange or oxidation to products other than combustion products.

The oxides selected for screening, along with their known functions described above, are listed in Table 1.

The results of the screening effort are summarized in Table 2, which compares the more selective systems at comparable conditions. Thallium(III) oxide and thallium(I) oxide were not screened in light of the Union Carbide work (*4*) and the high volatility, respectively (*10*), Thallium(III)

TABLE 2

Best Oxide Catalysts[a]

Oxide	mole CH_4 converted/mole metal · hr^{-1}		Selectivity[c]
	Total	To C_2+[b]	
Mn_2O_3/Mn_3O_4[d]	1.6	1.2	75
In_2O_3	1.6	1.2	75
GeO_2	0.33	0.23	70
SnO_2[d]	0.58	0.28	48
Bi_2O_3[d]	3.5	1.3	37
PbO[d]	1.1	0.88	80
Sb_2O_3[d]	3.2	2.3	72

[a] Nominal 5 wt% metal on SiO_2, 700°C, CH_4 GHSV = 860. Cumulative data were obtained during stoichiometric reduction of oxide. All oxides were regenerable by exposure to air.
[b] C_2+ is primarily (>90%) C_2H_4 and C_2H_6.
[c] mole CH_4 converted to C_2+/total CH_4 converted.
[d] Oxide is mentioned in Ref. (*4*).

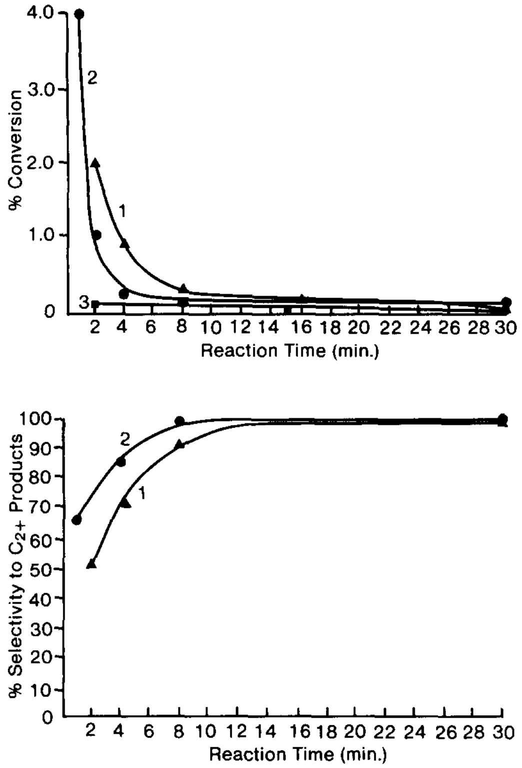

FIG. 1. Time dependence of instantaneous data for CH_4 over 5% Mn/SiO_2 at 600 GHSV and 700°C (1) and 800°C (2). Curve (3) is thermal conversion at 600 GHSV and 800°C over blank SiO_2.

oxide was one of several oxides tested in the Union Carbide work (*4*) using an inert quartz reactor and was reported to be selective. Of the oxides listed in Table 2, only manganese and tin showed no volatility problem over 6–12 redox cycles at 700–800°C. The others tended to vaporize out of the reactor, condensing downstream from the hot catalyst bed. At 700–800°C and methane GHSV = 600–800 hr^{-1}, reduction of the oxides was complete in 2 to 10 min. Figure 1 shows the reduction of the manganese–silica catalyst at 700 and 800°C. Also shown in Fig. 1 is the background thermal conversion over silica.

Manganese Systems

TABLE 3

Methane Conversion over 15% Mn/SiO_2 at 800°C and 600 GHSV

Run time (min)	% Conversion	% Selectivity					
		C_2H_4	C_2H_6	C_3	C_4–C_7	CO	CO_2
		Instantaneous results					
1[a]	30.1	36.5	13.9	2.2	3.6	19.5	24.2
2	12.3	42.9	27.0			17.0	12.9
12	.402	55.8	44.1				
30	.308	61.7	38.3				
		Cumulative results					
30[b]	2.27	31.8	23.9			15.8	28.3

[a] Catalyst productivity at 1 min = 0.16 g/g hr^{-1}.
[b] The selectivity to coke was less than 1%.

Because of its relative stability and activity the manganese system was selected for further study and optimization. Since the manganese oxide system is a stoichiometric reagent in this redox approach to methane conversion, the most obvious way to increase methane conversion under a given set of conditions is to increase manganese loading. Reagents of 5, 10, 15, 30, and 50 wt% manganese on silica were investigated. As seen in Fig. 2 an optimum manganese loading can be found. The results from the 15% manganese system are shown in Table 3. The high manganese loaded system, 50%, gave low catalyst productivities to higher hydrocarbons mainly because selectivities to carbon oxides were high. Indeed, similar results were obtained with the bulk oxides: MnO_2, Mn_2O_3, and Mn_3O_4. These results, along with the XRD analysis to be discussed later, show that a unique interaction between manganese and silica

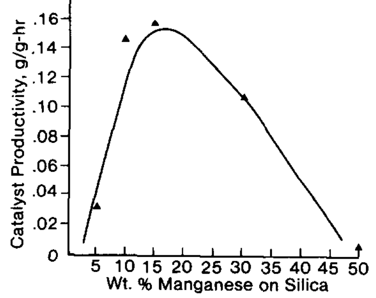

FIG. 2. One-minute instantaneous productivity (grams of C_{2+} produced per gram of catalyst per hour) as a function of Mn loading, at 800°C and 600 CH_4 GHSV.

must occur to form a selective conversion reagent.

Supporting evidence for this strong interaction is seen in the results with manganese supported on alumina. The previous work at Union Carbide (*4*) resulted in 45% C_2 selectivity at 11% methane conversion with 5% manganese on α-alumina. At similar manganese loadings and methane conversion we observed 20% C_{2+} selectivity when α-alumina was the support and 15% C_{2+} selectivity with γ-alumina. In the case of γ-alumina, the final catalyst had surface area similar to the 5% manganese on silica, 50–70 m^2/g. The silica catalysts show as high as 70% C_{2+} selectivity when run at 10% methane conversion. The reason for this large difference in support may be seen by XRD analysis.

Mechanism

Consideration of the overall mechanism can be conveniently divided into two parts, gas phase and solid phase. Gas phase reactions may be thought of as a carbon-building pyrolytic sequence, while the solid phase transition is the reduction of an oxide. This interpretation requires the inclusion of surface reactions at two points, the initial methane activation step and subsequent product oxidation to carbon oxides. While surface-catalyzed carbon-building reactions may occur, it is unnecessary to include them in the simplest interpretation of the results.

Solid phase. The net conversion of methane to higher hydrocarbons, carbon oxides, and water is the result of a redox reaction in which the solid oxidant is the limiting reagent. As the solid is reduced and the concentration of bound active oxygen decreases, the reaction rate falls, ultimately reaching the thermal background rate. Examples of the time dependence of the rate are shown in Fig. 1 and Table 3 for manganese on silica. The amount of carbon monoxide, carbon dioxide, and water formed in such runs corresponds to the quantity of available oxygen atoms. Since the manganese content is known, the ratio of active oxygen atoms to manganese atoms can be calculated and was found to be 0.4 ± 0.05. This ratio was confirmed by hydrogen reduction of the catalyst at 700–800°C in a Cahn microbalance. This could represent the reduction of Mn_3O_4 or Mn_7SiO_{12} to Mn(II) species. Both Mn_3O_4 and Mn_7SiO_{12} have been identified by XRD in the oxidized solid, while no crystalline species are evident in XRD of the reduced solid. The reduced solid is white, indicative of MnO, while the dark color of the oxidized solid is consistent with a higher oxide. MnO_2 decomposes in air above 550°C and can be ruled out. In the case of manganese on alumina, XRD revealed the formation of manganese aluminates. Clearly, the support effects involved here are not subtle ones; rather, they appear to arise from solid state reactions of the support with the metal.

Gas phase. Product selectivities are compared in Table 4 for methane runs over the better silica-supported systems and for methane pyrolysis in an empty tube, and over α-alumina, all under the same conditions. In the upper part of Table 4, the main differences in selectivities are the balances between hydrocarbons and carbon oxides and between carbon monoxide and carbon dioxide. No methanol or formaldehyde was observed. Of course, conversion is much higher over active oxides than in simple pyrolysis. In the lower part of Table 4, where hydrocarbon selectivities have been normalized to 100%, their trends as a function of carbon number are strikingly similar. In each case, C_2's predominate, while C_5's and toluene form minima in the distributions. If the carbon-building reactions occur to a significant extent on the surface, it is a remarkable coincidence that the hydrocarbon distribution produced over each metal oxide is so close to that produced by pyrolysis. On the contrary, it is probable that gas phase reactions are responsible for carbon building after methane activation at the surface. The differences noted above in carbon oxide selectivities indicate surface

TABLE 4

Instantaneous Results at 1 min into Run at 800°C and 860 GHSV

Catalyst (5 wt% metal)	% Methane conversion	% Selectivity								
		C_2H_4	C_2H_6	C_3	C_4	C_5	Benzene	Toluene	CO	CO_2
Bi/SiO_2	5.1	23.1	30.7	1.9	1.2	0.2	0.8	0.3	24.5	17.3
Ge/SiO_2	1.4	38.5	24.6	3.5	2.3	0.2	1.7	0.2	27.0	2.0
In/SiO_2	7.3	26.7	19.8	2.9	1.1	0.1	1.4	0.2	17.3	30.5
Mn/SiO_2	13.3	21.8	15.7	2.2	0.8	0.1	0.6	0.1	16.5	42.2
Pb/SiO_2	2.5	32.6	5.4	3.5	2.0	0.2	1.9	0.2	26.9	27.3
Sb/SiO_2	1.2	31.6	27.6	1.1	0.5	0.1	0.9	0.1	38.1	0.0
Sn/SiO_2	3.2	26.8	21.2	1.7	1.2	0.1	0.4	0.1	18.2	30.3
α-Al_2O_3	0.1	50.2	42.2	4.7	1.7	0.1	1.0	0.1	0.0	0.0
Empty tube	0.05	50.7	46.1	1.8	0.5	0.1	0.7	0.1	0.0	0.0
		Normalized hydrocarbon selectivity								
Bi/SiO_2		39.7	52.8	3.3	2.0	0.3	1.4	0.5		
Ge/SiO_2		54.2	34.7	4.9	3.2	0.3	2.4	0.3		
In/SiO_2		51.2	37.9	5.6	2.1	0.2	2.7	0.4		
Mn/SiO_2		52.8	38.0	5.3	1.9	0.2	1.5	0.2		
Pb/SiO_2		71.2	11.8	7.6	4.4	0.4	4.2	0.4		
Sb/SiO_2		51.1	44.6	1.8	0.8	0.1	1.4	0.2		
Sn/SiO_2		52.0	41.1	3.3	2.3	0.2	0.8	0.2		
α-Al_2o_3		50.2	42.2	4.7	1.7	0.1	1.0	0.1		
Empty tube		50.7	46.1	1.8	0.5	0.1	0.7	0.1		

participation in their production. Product degradation, e.g., allylic oxidation of olefins, is a reasonable route to carbon oxides. An alternative route is coking of olefins and aromatics on the oxidizing surface where most of the coke is subsequently converted to carbon oxides. As another possibility, the solid oxide may thermally decompose to give enough gas phase oxygen to account for both product oxidation and methane activation. This possibility can be ruled out because oxide decomposition is far too slow to provide the amount of oxygen-containing products observed. It is this fact that makes it possible to flush the reactor with nitrogen for durations of 1 to 30 min after air oxidation with no decrease in activity in the subsequent methane run. Trace oxygen can be observed in the reactor effluent during the nitrogen flush, but it would take at least 10 hr to supply enough oxygen by thermal decomposition to form the products observed during a 2-min methane run.

A series of methane runs was carried out on manganese oxide on silica over a range of reactor residence times to determine the sequence of product formation. Figure 3 shows the dependence of product selectivities and methane conversion on residence time. Carbon monoxide, carbon dioxide, and coke are plotted together for simplicity. Coke accounts for no more than 2% selectivity in these runs. Carbon monoxide is slightly more persistent than carbon dioxide as residence time decreases, but the difference is not significant enough to unequivocally indicate stepwise formation of the dioxide from the monoxide. Carbon oxides taken as a whole do appear, for the most part, to be secondary products. The same is true for ethylene, C_3 products (mostly propylene), C_4 products (mostly butadiene), C_5 (mostly diolefins), benzene, and toluene. The latter three products, most of which is benzene, amount to only 1% selectivity at the longest residence time. The only product displaying increasing selectivity with decreasing residence time is

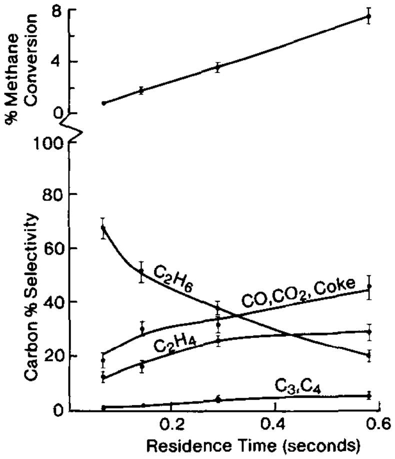

FIG. 3. One-minute cumulative data for CH_4 feed over 5% Mn/SiO_2 at 800°C.

ethane, leading to its identification as the primary product with a lifetime greater than 0.1 sec. Ethylene can be formed from ethane by thermal and oxidative dehydrogenation. Under conditions reported here, these two processes have been observed and found to have rates of the same order of magnitude. The only reasonable mechanism for ethane formation is the removal of a hydrogen atom from methane by the solid oxide, leaving a methyl radical species and a surface hydroxyl group, followed by methyl radical recombination to ethane and addition of another hydrogen atom from a second methane to the surface to form water which is subsequently desorbed. Methyl radicals play a similar role in ethane formation from methane–oxygen cofeed (*8*). Whether the methyl radicals remain bound to the surface until recombination or recoil immediately to the gas phase is an unresolved question, the answer to which depends in part on the extrapolation of the curves in Fig. 3 to zero residence time. Such an extrapolation indicates, at most, a minor role for methyl radical oxidation; the majority of methyl radicals apparently form ethane. To the extent that extrapolations for ethylene and carbon oxides approach zero, and that for ethane 100%, they favor the gas phase mechanism. A surface-bound methyl radical would face some probability of forming a surface methoxy group and subsequently carbon monoxide, which would appear at zero residence time. If ethane were formed on the surface, a rapid oxidative dehydrogenation would be possible prior to ethane desorption, leaving some nonzero ethylene selectivity at zero residence time. In fact, in separate experiments using ethane feed over this solid oxide, oxidative dehydrogenation was observed to have a faster rate than the analogous reaction on methane, in conformity to the lower CH bond energy of ethane.

Further evidence for the participation of methyl radicals comes from two other series of runs, with mixed feeds of 5 mole% ethylene in methane and 5 mole% propylene in methane, in which residence time was varied over the same range as in the pure methane runs. In the methane–ethylene case, propylene and butene appear to be primary products, while ethane falls away at the shortest residence time as shown in Fig. 4. Ethylene dimerization would produce butene as a primary product. Addition of a methyl radical to ethylene (*11*) and subsequent elimination of a

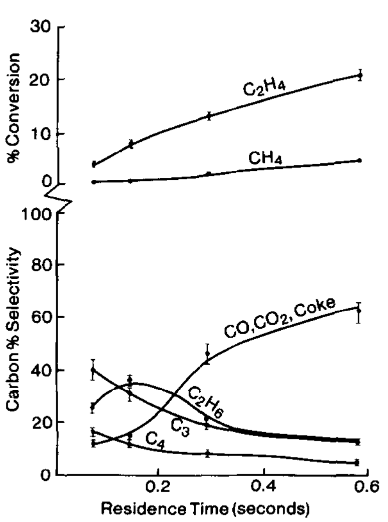

FIG. 4. One-minute cumulative data for a feed of 5 vol.% C_2H_4 in CH_4 over 5% Mn/SiO_2 at 800°C.

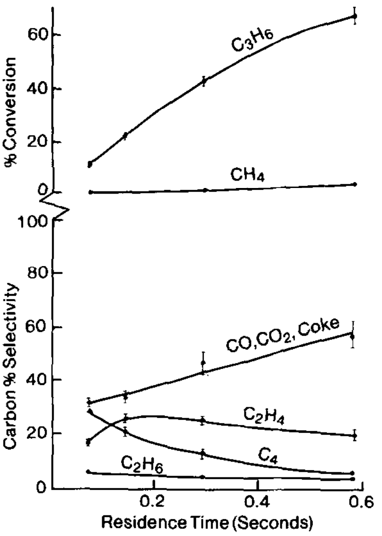

FIG. 5. One-minute cumulative data for a feed of 5 vol.% C_3H_6 in CH_4 over 5% Mn/SiO_2 at 800°C.

hydrogen atom to yield propylene (*12*) are known to be rapid gas phase reactions. This is consistent with production of propylene as a primary product. In the case of methane–propylene as shown in Fig. 5, ethane persists at short residence times, but only butene shows a strong upward trend. Butene could arise as a primary product by way of methyl addition to propylene (*13*), in analogy to the methane–ethylene case. If addition of methyl to olefin feed components is taking place, then such oligomerization could proceed to still heavier products, which could in turn crack back to light products, thus masking the actual primary product distribution. Such sequential reactions would, however, contribute less to the C_3 and C_4 selectivities under consideration here as residence time decreases.

An alternate explanation for the enhanced C_3 and C_4 product from mixed feeds, simple pyrolysis or oxidative conversion of the olefin feed component with no contribution from methane, was eliminated. Runs were made with 5 vol.% olefin in nitrogen over both oxidized and reduced manganese on silica. The rate of C_3 production was several times greater for mixed 95% methane–5% ethylene than the sum of C_3 produced separately in runs of methane and 5% ethylene in nitrogen, over both oxidized and reduced solids. C_4 production, on the other hand, was only slightly faster for the mixed feed than 5% ethylene over an oxidized solid, and was the same rate over a reduced solid. This supports the idea that, in this case, C_4 production is largely from ethylene dimerization. C_4 production from mixed methane–propylene was greater than that from the sum of separate methane and 5% propylene in nitrogen feeds, over both oxidized and reduced solids. For both mixed feeds, coupling of feed components was faster over the oxidized solid than the reduced solid. Methyl radical addition to olefins and enhanced methyl radical yields via oxidation can explain all of these observations.

The basic gas phase and surface steps of a satisfactory mechanism are summarized below:

$$CH_4 + MnO_x \rightarrow CH_3 + MnO_xH$$

$$2MnO_xH \rightarrow MnO_x + MnO_{x-1} + H_2O$$

$$2CH_3 \rightarrow C_2H_6$$

$$C_2H_6 \rightarrow C_2H_4 + H_2$$

$$H_2 + MnO_x \rightarrow H_2O + MnO_{x-1}$$

$$C_2H_6 + MnO_x \rightarrow C_2H_4 + H_2O + MnO_{x-1}$$

$$2C_2H_4 \rightarrow C_4H_8$$

$$CH_3 + C_2H_4 \rightarrow C_3H_6 + H$$

$$CH_3 + C_3H_6 \rightarrow C_4H_8 + H$$

$$H + H \rightarrow H_2$$

$$\text{Olefins} \xrightarrow{MnO_x} CO, CO_2$$

$$\text{Olefins} \rightarrow \text{coke} \xrightarrow{MnO_x} CO, CO_2$$

CONCLUSIONS

A number of silica-supported metal oxides have been identified which are capable of selectively converting methane to ethylene and higher hydrocarbons. From a practical standpoint, high product yields require operating temperatures of at least 800°C, which eliminates many otherwise promising metal oxides from consideration due to their volatility. Under this constraint, the manganese–silica system is the most attractive. Instantaneous hydrocarbon product yields as high as 17% at 56% selectivity have been obtained. The primary function of the metal oxide appears to be the oxidation of methane to methyl radicals and water. The methyl radicals subsequently undergo a series of thermal reactions to form higher carbon number products. Nonselective products, carbon oxides and coke, appear to arise principally from product degradation rather than directly from methane. The simultaneous reduction of the solid is less well understood. In the case of manganese–silica the species responsible for selective oxidation may be a manganese silicate or manganese oxide perturbed by a strong support interaction. If systems cannot be found which are active at lower temperature, significant improvement will only come with modification of the solid oxides to suppress product oxidation.

ACKNOWLEDGMENTS

The authors wish to thank Mr. William S. Brown and Mr. Alex Neill for technical assistance and Ms. Barbara A. King for catalyst characterization.

REFERENCES

1. Chamberlin, D. S., and Bloom, E. B., *Ind. Eng. Chem.* **21,** 945 (1929).
2. Happel, J., and Kramer L., *Ind. Eng. Chem.* **59,** 39 (1967).
3. Mitchell, H. L., III, and Waghorne, R. H., U.S. Patents 4,172,810 (1979); 4,205,194 (1980); and 4,239,658 (1980) to Exxon Res. and Eng. Co.
4. Keller, G. E., and Bhasin, M. M., *J. Catal.* **73,** 9 (1982).
5. Jones, C. A., Leonard, J. J., and Sofranko, J. A., U.S. Patents 4,443,644; 4,443,645; 4,443,646; 4,443,647; 4,443,648; 4,443,649; and 4,444,984 to Atlantic Richfield Co. (1984).
6. Margolis, L. Y., *in* "Advances in Catalysis" (D. D. Eley, H. Pines, and P. B. Weisz, Eds.), Vol. 14, p. 429. Academic Press, New York, 1963; Cullis, C. F., Keene, D. E., and Trimm, D. L., *J. Catal.* **19,** 378 (1970); Andrushkevich, T. V., Popovskii, V. V., and Boreskov, G. K., *Kinet. Katal.* **6,** 860 (1965).
7. Hinsen, W., and Baerns, M., *Chem. Ztg.* **107,** 223 (1983).
8. Ito, T., Wang, J. X., Lin, C. H., and Lunsford, J. H., *J. Amer. Chem. Soc.* **107,** 5062 (1985).
9. Otsuka, K., Jinno, K., and Morikawa, A., *Chem. Lett.* 499 (1985).
10. Trimm, D. L., and Doerr, L. A., *J. Catal.* **23,** 49 (1971).
11. Camilleri, P., Marshall, R. M., and Purnell, H., *J. Chem. Soc. Faraday Trans. I* **71,** 1491 (1975).
12. Sundaram, K. M., and Froment, G. F., *Ind. Eng. Chem. Fundam.* **17,** 174 (1978).
13. Cretanović, R. J., and Irwin, R. S., *J. Chem. Phys.* **46,** 1694 (1967).